21th International Conference on Renewable Energies and Power Quality (ICREPQ'23)
Madrid (Spain), 24th to 26th May 2023
Renewable Energy and Power Quality Journal (RE&PQJ)
ISSN 2172-038 X, Volume No.21, July 2023

Use of building façade for active indoor humidity control

Kamel Ghali, Jean Paul Harrouz, Nesreen Ghaddar
Department of Mechanical Engineering, Faculty of Engineering and Architecture, American University of Beirut, Beirut, Lebanon
P.O. Box 11-0236, Beirut 1107-2020, Lebanon
Phone/Fax number: +961 1 340 460, e-mail: ka04@aub.edu.lb, jeh15@mail.aub.edu, farah@aub.edu.lb

MOTIVES AND INCENTIVES

Providing a healthy environment within indoor spaces is thus crucial to protect the occupants' wellbeing. Such environments are created by maintaining indoor generated species such water vapor, CO_2, and VOCs to ensure good air quality. Among these species, careful consideration should be given to the indoor H_2O levels. Conventionally, humidity control is carried out by pumping dehumidified air into the space to dilute the indoor-generated moisture. Such techniques rely on the use of vapor compression cooling either as standalone systems or integrated with desiccant dehumidifiers to generate this dried air. These methods are known to be energy intensive, especially in hot and humid climates. Recent efforts are made to directly remove the indoor moisture using hygroscopic materials. These materials act as moisture buffers and can reduce the fluctuations in indoor RH levels. However, they suffered from limited capacity and a batch operation that requires complex switching mechanism. Another approach for direct humidity control would be to exploit the building structure to drive the humidity outdoors. Most building façades are of a breathable nature, which facilitates moisture transfer. This technique relies thus on the gradient in the water vapor pressure between the indoor and outdoor air as driver for the moisture flow. Accordingly, this approach has been applied only to dry climates to avoid the reversal of the moisture flow from outdoor environment to the indoor space. Nevertheless, its applicability has been expanded to humid regions by pumping dry air into the building structure. Such system used a rotating bed packed with MOFs based desiccant to dehumidify the outdoor air and supply it the building façade. This created the needed driving gradient for the moisture transfer from the indoor space, irrespective of the outdoor air conditions. It is important to study the performance of this system under extreme weather conditions to determine its range of applicability.

SYSTEM DESCRIPTION

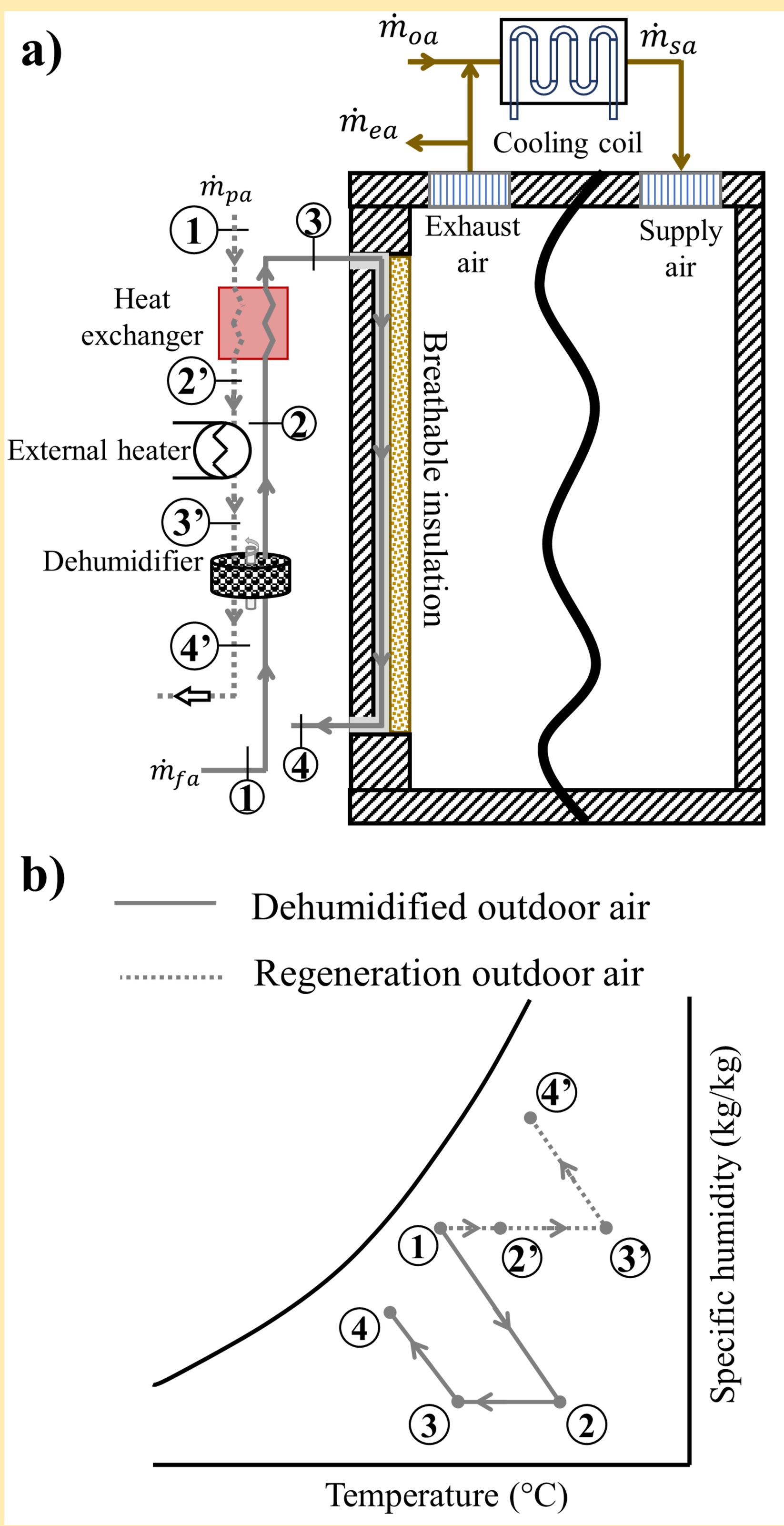

Fig. 1. Schematic of a) proposed system and b) psychrometric chart of the process outdoor air flowrates.

The proposed system is implemented in an office space located in a hot and humid climate. The space relative humidity levels are maintained at 60 % using the proposed system that consists of three main components as shown in Fig. 1(a): a rotating packed bed, a breathable ventilated façade, and an air-to-air heat exchanger. The rotating packed bed employ MOFs-based desiccant to dehumidify the outdoor air. The building façade consist of an airgap whose indoor side is formed of a breathable insulation. The latter enable the reduction of the sensible heat gain into the space from the hot dried outdoor air without hindering moisture transfer. The air-to-air heat exchanger is used to cool the dried outdoor air before it is introduced into the façade to reduce the sensible heat gains to the space.

The system operation is thus summarised as follows: the outdoor air at flowrate ($\dot{m}_{fa}$) at state (1) enters the desiccant dehumidifier. The resulting hot and dry air at state (2) is cooled with the outdoor air in the heat exchanger to state (3) before it is introduced in the airgap. The dry air picks up the moisture transferred from the indoor space before it is discharged to the outdoors at state (4). Simultaneously, the outdoor air at a flowrate of ($\dot{m}_{pa}$) is used to regenerate the desiccant. It is thus preheated in the heat exchanger from state (1) to state (2') before it enters the external heater to reach the regeneration temperature (T_{reg}) at state (3').

The regeneration airflow is then discharged to the outdoor at state (4') with the purged water vapor. The different air states are shown on the psychrometric chart of Fig. 1(b). Note that a third stream of outdoor air at a flowrate of ($\dot{m}_{oa}$) is mixed with the room return air before they are cooled to the required supply temperature (T_{sup}) and pumped into the space at a flowrate of ($\dot{m}_{sa}$) to meet the required temperature and CO_2 levels in the office.

CASE STUDY

The system performance is evaluated for a case study of a typical four-workers office space of (5 m × 5 m × 3 m) located in Jeddah, KSA. The proposed system is installed on one of the office façades and its area is fixed at 50 % of the wall area, with a height of 2 m while the airgap is set to 2 cm. To ensure an effective mass transfer, the air velocity is set to 1.5 m/s. The rotating packed bed is sized to hold the maximum amount of water to be removed from outdoor air. Having these conditions, the needed adsorbent mass to remove the latent load in the proposed and conventional systems are 2.5 kg and 20 kg of MIL-101-Cr beads, respectively. The corresponding bed diameter and length are 0.35 m and 0.15 m for the proposed system while for the conventional system, they are set to 0.7 m and 0.25 m, respectively. Accordingly, an initial saving of 89 % was achieved using the proposed system.

METHODOLOGY

Mathematical models are developed for the heat and mass transfer in the airgap of the ventilated façade and in the desiccant dehumidifier. The models are used to size and optimize the system operation to meet the required indoor moisture levels.

The air in the ventilated façade exchange both heat and water vapor with the indoor air through the breathable insulation. Since the used mineral wool insulation has a negligible water vapor uptake, a steady one-dimensional couple heat and mass transfer model is adopted. The resulting energy and mass balances for the airgap are given by the equivalent resistance scheme

$$\frac{dT_{oa}}{d\bar{z}} = \frac{U_H A_{ins}}{\dot{m}_{oa} C_{p,oa}} \left(1 + \frac{C_{p,wv}}{C_{p,oa}} (\omega_{ia} - \omega_{oa})\right) (T_{ia} - T_{oa})$$

$$\frac{d\omega_{oa}}{d\bar{z}} = \frac{U_M A_{ins}}{\dot{m}_{oa}} (\omega_{ia} - \omega_{oa})$$

The rotating and fixed packed beds share similarity in terms of desiccant configuration and airflow patterns. Moreover, the low rotational speed of the rotating packed bed, radial air convection can be neglected. Hence, a transient one-dimensional coupled heat and mass transfer between the airflow and the desiccant. The water vapor mass balance for the air stream is thus given by

$$\varepsilon_s \rho_{oa} \frac{\partial \omega_{oa}}{\partial t} + \rho_{oa} u_{oa} \frac{\partial \omega_{oa}}{\partial y} - D_{v,s} \frac{\partial^2 \omega_{oa}}{\partial y^2} + (1 - \varepsilon_s) \rho_s \frac{\partial \bar{q}_s}{\partial t} = 0$$

For the solid side mass transfer, the linear driving force (LDF) model is adopted where the film, micro- and macropore mass transfer resistances are lumped into a single term, the LDF time constant. The water vapor mass balance is given by

$$\frac{\partial \bar{q}_s}{\partial t} = k_{LDF} (\bar{q}^*{}_s - \bar{q}_s)$$

The different models are integrated in a MATLAB code where the different heat and mass balances are solved using the finite volume approach with implicit first order upwind scheme. A time step independence test yielded a time step of 10^{-5} s that is adopted to ensure accurate results with acceptable computational time. The convergence criterion is met when the difference between two different iteration is lower than the tolerance of 10^{-8} for all the calculated parameters.

RESULTS AND DISCUSSION

The developed mathematical models were validated for different air conditions in the airgap and the maximum discrepancies were less than 10 % for all calculated parameters of both the ventilated airgap and desiccant dehumidifier models.

The validated models were then used to properly operate the proposed system. For this reason, the outdoor air flowrates ṁfa and ṁsa entering the dehumidifier in both proposed and conventional systems were determined to maintain the indoor air conditions specified in Section 2 during the peak humidity month of August as shown in Fig. 2(a). The corresponding electrical energy for the fan operation (Ee,f), vapor compression cooling coil (Ee,c) as well as the regeneration thermal energy (Et) are shown in Fig. 2(b-c).

The dehumidified outdoor air flowrate in the proposed system ($\dot{m}_{fa}$) varied with the outdoor air specific humidity. It increased from 0.11 kg/s around noon hours where the outdoor humidity was at the lowest values of 22.8 g/kg and reached 0.14 kg/s at peak humidity of 25.4 g/kg (Fig. 1(a)). On the other hand, the dehumidified outdoor air in the conventional system consisted of the space supply flowrate ($\dot{m}_{sa}$). Accordingly, this flowrate was dictated by the space cooling load and followed its hourly variation pattern. It increased from 0.85 kg/s during early hours of the day when the outdoor conditions of temperature and radiation were low and reached 1.82 kg/s at 16:00 hr at the peak load hour (Fig. 1(a)). The proposed system operation required thermal energy that varied between 0.49 kWh and 0.7 kWh fan electrical energy between 0.31 kWh and 0.6 kWh and coil electrical energy between 2.1 kWh and 3.85 kWh (Fig. 2(b)). The first two parameters followed the pattern of $\dot{m}_{fa}$ whereas the last one followed the cooling load of the office space. On the other hand, the thermal and electrical energy consumption of the conventional system was higher by two orders of magnitude.

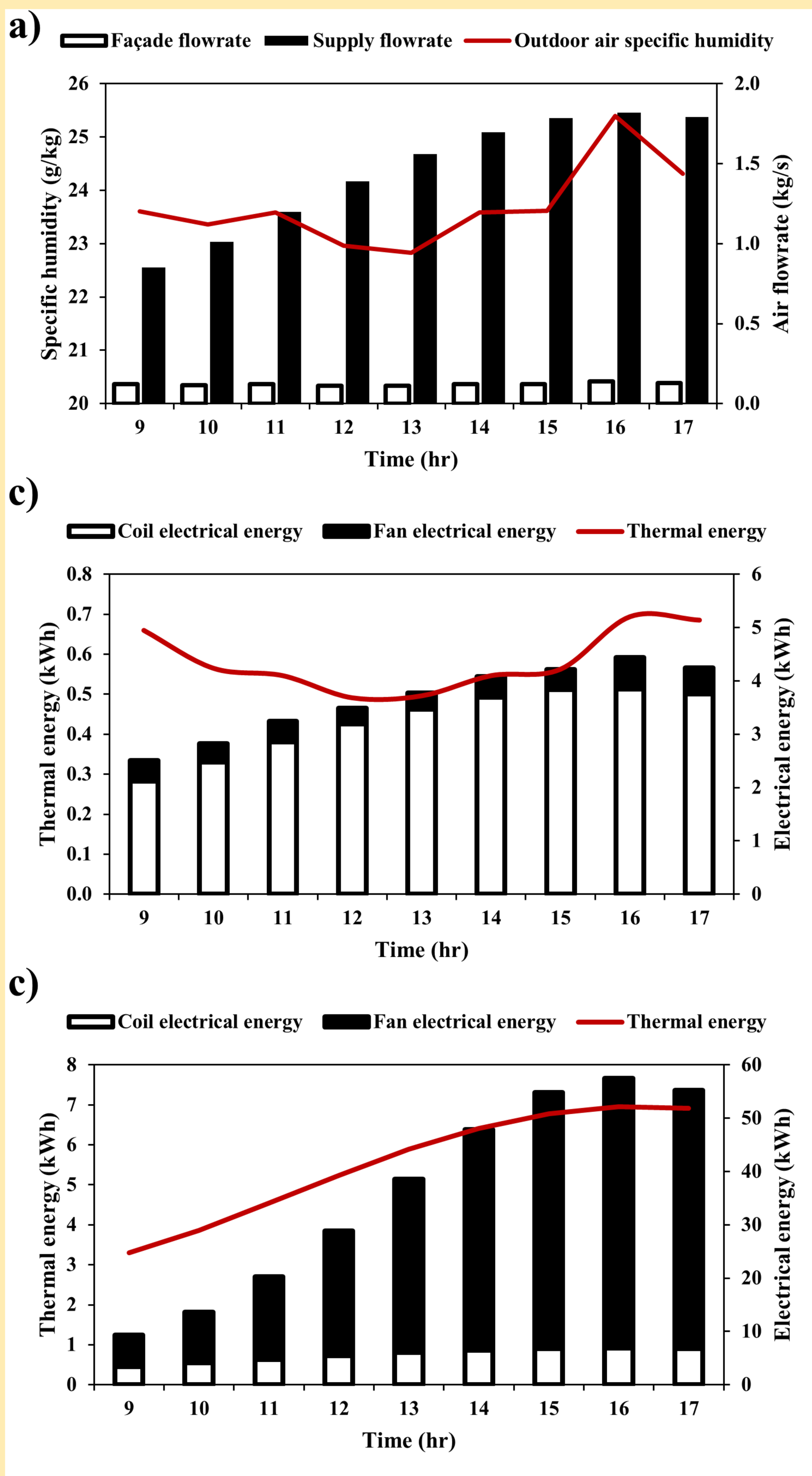

Fig. 2. The obtained a) outdoor air flowrate entering the dehumidifier and the corresponding energy consumption for b) the proposed and c) conventional systems.

They varied between 3.3 kWh and 7 kWh for E_t and 5.9 kWh and 50.6 kWh for $E_{e,f}$ (Fig. 2(c)). This was due to the relatively higher outdoor air flowrate treated in the dehumidifier that necessitated higher thermal energy for regeneration and high electrical energy to drive the fan. On the other hand, the electrical energy needed for the cooling coil varied within the same order of magnitude and increased from 3.4 kWh to 7 kWh with the increase in the space load. The highest reduction was achieved at the level of the fan electrical energy, which reached 98 %. On the other hand, the proposed system achieved a reduction of 89.5 % in the thermal energy and 42 % reduction in the cooling coil energy. Assuming an electricity cost of 0.13 USD/kWh and a thermal energy cost of 0.019 USD/kWh, the proposed system resulted in a reduction of 90 % in the operating cost of the office space humidity control system compared to the conventional system during the peak humidity month.

CONCLUSION

Over the peak humidity month of August, the proposed system reduced by 89 % and 90 % the system size and operating cost, respectively, compared to the conventional system employing vapor compression cooling integrated with desiccant dehumidifier. This indicates that as the outdoor humidity increased, the savings obtained by the proposed system increased as well.